

Phosphodiester Hydrolysis by a New Zinc(II) Macrocyclic Tetraamine Complex with an Alcohol Pendant: Elucidation of the Roles of Ser-102 and Zinc(II) in Alkaline Phosphatase

Eiichi Kimura,^{*,†} Yorimitsu Kodama,[†] Tohru Koike,[†] and Motoo Shiro[‡]

Contribution from the Department of Medicinal Chemistry, School of Medicine, Hiroshima University, Kasumi 1-2-3, Minami-ku, Hiroshima 734, Japan, and Rigaku Corporation, Matsubaracho 3-9-12, Akishima, Tokyo 196, Japan

Received March 28, 1995[⊗]

Abstract: A new benzyl alcohol-pendant 1,4,7,10-tetraazacyclododecane (cyclen) ligand, (*S*)-1-(2-hydroxy-2-phenylethyl)-1,4,7,10-tetraazacyclododecane (L) (**11**), has been synthesized. The complexation of **11** with Zn^{II} yielded 1:1 five-coordinate complexes (isolated as its perchlorate salts with the pendant alcohol either undissociated (ZnL, **14a**) or dissociated (ZnH₂L, **14b**) from acidic (pH 6.0) or basic (pH 9.5) aqueous solution, respectively). The p*K*_a value for the pendant alcohol (**14a** ⇌ **14b** + H⁺) was determined by potentiometric pH titration to be 7.30 ± 0.02 at 35 °C with *I* = 0.10 (NaNO₃). The X-ray crystal study of **14b** has shown two crystallographically distinct structures with the alkoxide closely coordinated at the fifth coordination site, where an average distance of Zn–O[−] is 1.91 Å. Crystals of **14b**·ClO₄ (C₁₆H₂₇N₄O₅ClZn) are orthorhombic, space group *P*2₁2₁2₁ (no. 19) with *a* = 16.977 (4) Å, *b* = 18.135 (4) Å, *c* = 13.173 (3) Å, *V* = 4055 (1) Å³, *Z* = 8, *R* = 0.050, and *R*_w = 0.077. The Zn^{II}-bound alkoxide anion in **14b** is a more reactive nucleophile than *N*-methylcyclen-Zn^{II}–OH[−] species **15b**. In the kinetic study using **14** in aqueous solution (pH 6.0–10.3) at 35 °C with *I* = 0.10 (NaNO₃), the rate–pH profile for a phosphoryl transfer reaction from bis(4-nitrophenyl) phosphate (BNP[−]) to **14b** gave a sigmoidal curve with an inflection point at pH 7.4, which corresponds to the p*K*_a value for **14a** ⇌ **14b** + H⁺. The second-order rate constant *k*_{BNP} of (6.5 ± 0.1) × 10^{−4} M^{−1} s^{−1} is 125 times greater than the corresponding value of (5.2 ± 0.2) × 10^{−6} M^{−1} s^{−1} for BNP[−] hydrolysis catalyzed by **15b**. The product of the phosphoryl transfer reaction from BNP[−] to **14b** is the pendant alcohol-phosphorylated **16**, which was isolated as its perchlorate salt **16a** by reacting **14b** with BNP[−] in DMF. In anhydrous DMF solution, the phosphoryl transfer (*k*_{BNP} of 1.1 ± 0.1 M^{−1} s^{−1} at 35 °C) is 1700 times faster than that in aqueous solution. In the subsequent reaction of **16**, the pendant phosphodiester undergoes an intramolecular nucleophilic attack by the Zn^{II}-bound OH[−] of **16b** to yield a phosphomonoester product **17**. From the sigmoidal rate–pH relationship (pH 7.4–10.5), the kinetic p*K*_a value of 9.0 was estimated for **16a** ⇌ **16b** + H⁺, which is almost the same value (p*K*_a = 9.10 ± 0.05) determined by potentiometric pH titration at 35 °C. The first-order rate constant for the reaction **16b** → **17** is (3.5 ± 0.1) × 10^{−5} s^{−1} at 35 °C with *I* = 0.10 (NaNO₃). As a reference to this intramolecular phosphodiester hydrolysis, ethyl (4-nitrophenyl) phosphate (NEP[−]) was hydrolyzed by **15b**. The second-order rate constant *k*_{NEP} was (7.9 ± 0.3) × 10^{−7} M^{−1} s^{−1} at 35 °C with *I* = 0.10 (NaNO₃). Thus, the intramolecular hydrolysis is 45 000 times faster than the intermolecular NEP[−] hydrolysis with 1 mM **15b**. The present findings that demonstrate the potential of the proximate alcohol by Zn^{II} in the initial phosphoryl transfer and the potential of the Zn^{II}-bound water in the intramolecular phosphate hydrolysis may well serve to elucidate the collaborative functions of Ser-102 and Zn^{II} ions in alkaline phosphatase.

Introduction

Alkaline phosphatase (AP) is a Zn^{II}-containing enzyme that nonspecifically hydrolyzes phosphate monoesters (ROPO₃^{2−}) at alkaline pH.¹ Intensive studies have been done on *E. coli* alkaline phosphatase. On the basis of X-ray structure² and NMR study³ of native and metallo-substituted AP, it is now accepted that, at the AP active center consisting of two Zn^{II} ions (ca. 4 Å separation), a substrate monophosphate is initially attacked by Ser-102 in **1** to yield a phosphoseryl–enzyme intermediate **2**, which subsequently is attacked by the adjacent Zn^{II}–OH[−] to complete the hydrolysis **3** → **4** and reproduce the free form of serine to reinitiate the catalytic cycle (see Scheme 1).⁴

In Scheme 1, the A-site Zn^{II} serves to coordinate the phosphate substrate to make it vulnerable to the attack of Ser-102 that is potentiated by the B-site Zn^{II} (**1**). After the phosphate is transferred from the substrate to Ser-102 (**2**), the vacated coordination site of the A-site Zn^{II} activates an H₂O as Zn^{II}–OH[−], which becomes an intramolecular nucleophile in the final dephosphorylation (**3** → **4**). The wild-type AP reaches maximal activity around pH 8, where the rate-limiting step is release of the tightly bound inorganic phosphate (the product) from the enzyme–product complex **4**. Accordingly, inorganic phosphate is a competitive inhibitor. At pH < 5.5, the phosphoseryl intermediate **2** is stable.^{3d,5}

There are some intrinsic questions concerning the AP mechanism, such as (i) what is the special advantage in forming the phosphoseryl intermediate **2** for indirect hydrolysis and (ii) how does the Ser-102 associated with the Zn^{II} ion become a nucleophile? Recently, the Ser-102 in AP was replaced using site-directed mutagenesis by Leu and Ala.⁶ The mutant enzymes still catalyzed the phosphate hydrolysis, with similar rate–pH

[†] Hiroshima University.

[‡] Rigaku Corp.

[⊗] Abstract published in *Advance ACS Abstracts*, August 1, 1995.

(1) Coleman, J. E. *Annu. Rev. Biophys. Biomol. Struct.* **1992**, *21*, 441–483.

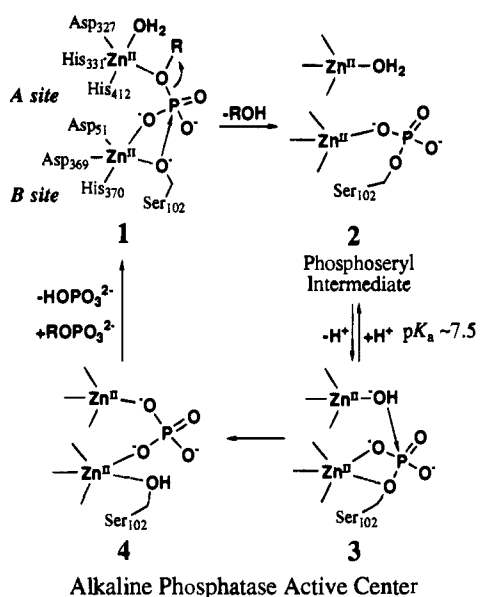
(2) Kim, E. E.; Wyckoff, H. W. *J. Mol. Biol.* **1991**, *218*, 449–464.

(3) (a) Gettins, P.; Coleman, J. E. *J. Biol. Chem.* **1984**, *259*, 4991–4997. (b) Hull, W. E.; Halford, S. E.; Gutfreund, H.; Sykes, B. D. *Biochemistry* **1976**, *15*, 1547–1561. (c) Bock, J. L.; Cohn, M. *J. Biol. Chem.* **1978**, *253*, 4082–4085. (d) Coleman, J. E.; Gettins, P. *Zinc Enzymes*; Birkhäuser: Boston, MA, 1986; Chapter 6, p 77.

(4) For a review: Fenton, D. E.; Okawa, H. *J. Chem. Soc., Dalton Trans.* **1993**, 1349–1357.

(5) Ried, T. W.; Wilson, L. B. *Enzyme* **1971**, *4*, 373–415.

Scheme 1



profiles, although the catalytic efficiency is 1/500 to 1/1000 of that of the wild-type enzyme, for which the direct hydrolysis of the substrate by Zn^{II}-OH⁻ was proposed. In other hydrolytic metalloenzymes, the direct hydrolysis by M-OH⁻ species seems more prevalent.⁷

There have been numerous studies of phosphatase model systems using simple metal complexes,^{8,9} but most of these models have been built for the sole M-OH⁻ systems as nucleophiles, while few were concerned with the net reaction initiated by the metal-bound alcohol, followed by the metal-bound water, as was revealed by AP.

Recently, we discovered that Zn^{II}-1,5,9-triazacyclododecane ([12]aneN₃) complex **5a**^{10,11} and Zn^{II}-1,4,7,10-tetraazacyclododecane (cyclen) complex **6a**¹² can activate an H₂O as the Zn^{II}-bound OH⁻ species **5b** (pK_a = 7.3) and **6b** (pK_a = 7.9)

(6) Butler-Ransohoff, J. E.; Rokita, S. E.; Kendall, D. A.; Banzon, J. A.; Carano, K. S.; Kaiser, E. T.; Matlin, A. R. *J. Org. Chem.* **1992**, *57*, 142-145.

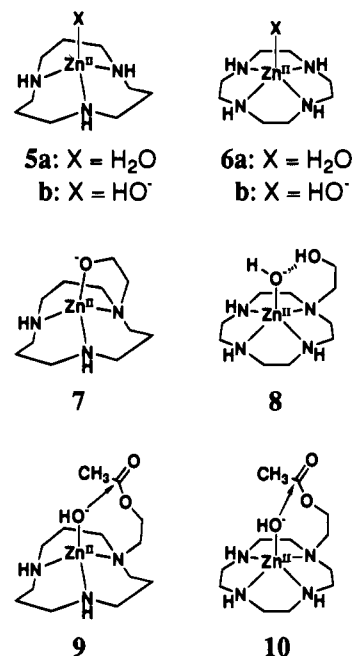
(7) (a) Mueller, E. G.; Crowder, M. W.; Averill, B. A.; Knowles, J. R. *J. Am. Chem. Soc.* **1993**, *115*, 2974-2975. (b) Coleman, J. E. *Zinc Enzymes*; Birkhäuser: Boston, MA, 1986; Chapter 4, p 49.

(8) For a review of bimetallic enzyme models: (a) Göbel, M. W. *Angew. Chem., Int. Ed. Engl.* **1994**, *33*, 1141-1143. (b) Karlin, K. D. *Science* **1993**, *261*, 701-708.

(9) (a) For Ir^{III} complexes: Hendry, P.; Sargeson, A. M. *J. Am. Chem. Soc.* **1989**, *111*, 2521-2527. (b) For Co^{III} complexes: Jones, D. R.; Lindoy, L. F.; Sargeson, A. M. *J. Am. Chem. Soc.* **1983**, *105*, 7327-7336. Hendry, P.; Sargeson, A. M. *Inorg. Chem.* **1990**, *29*, 92-97. Chin, J.; Banaszczuk, M.; Jubian, V.; Zou, X. *J. Am. Chem. Soc.* **1989**, *111*, 186-190. Kim, J. H.; Chin, J. *J. Am. Chem. Soc.* **1992**, *114*, 9792-9795. Connolly, J. A.; Banaszczuk, M.; Hynes, R. C.; Chin, J. *Inorg. Chem.* **1994**, *33*, 665-669. (c) For Ln^{III} complexes: Schneider, H.-J.; Rammo, J.; Hettich, R. *Angew. Chem., Int. Ed. Engl.* **1993**, *32*, 1716-1719. Hay, R. W.; Govan, N. *J. Chem. Soc., Chem. Commun.* **1990**, 714-715. Morrow, J. R.; Buttrey, L. A.; Shelton, V. M.; Berback, K. A. *J. Am. Chem. Soc.* **1992**, *114*, 1903-1905. Chin, K. O. A.; Morrow, J. R. *Inorg. Chem.* **1994**, *33*, 5036-5041. Tsubouchi, A.; Bruce, T. C. *J. Am. Chem. Soc.* **1994**, *116*, 11614-11615. (d) For Zn^{II} complexes: Sigman, D. S.; Jorgensen, C. T. *J. Am. Chem. Soc.* **1972**, *94*, 1724-1731. Gellman, S. H.; Petter, R.; Breslow, R. *J. Am. Chem. Soc.* **1986**, *108*, 2388-2394. Hikichi, S.; Tanaka, M.; Moro-oka, Y.; Kitajima, N. *J. Chem. Soc., Chem. Commun.* **1992**, 814-815. Ruf, M.; Weis, K.; Vahrenkamp, H. *J. Chem. Soc., Chem. Commun.* **1994**, 135-136. (e) For Fe^{III} complexes: Wilkinson, E. C.; Dong, Y.; Que, L. Jr. *J. Am. Chem. Soc.* **1994**, *116*, 8394-8395.

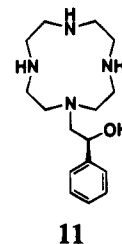
(10) (a) Kimura, E.; Shiota, T.; Koike, T.; Shiro, M.; Kodama, M. *J. Am. Chem. Soc.* **1990**, *112*, 5805-5811. (b) Kimura, E.; Koike, T.; Shionoya, M.; Shiro, M. *Chem. Lett.* **1992**, 787-790. (c) Koike, T.; Kimura, E. *J. Am. Chem. Soc.* **1991**, *113*, 8935-8941. (d) Zhang, X.; van Eldik, R.; Koike, T.; Kimura, E. *Inorg. Chem.* **1993**, *32*, 5749-5755. (e) Koike, T.; Kimura, E.; Nakamura, I.; Hashimoto, Y.; Shiro, M. *J. Am. Chem. Soc.* **1992**, *114*, 7338-7345. (f) Kimura, E.; Shionoya, M.; Hoshino, A.; Ikeda, T.; Yamada, Y. *J. Am. Chem. Soc.* **1992**, *114*, 10134-10137.

and that both catalyze hydrolysis of carboxyesters,^{10a-c} β-lactams,¹² phosphotriesters, and phosphodiester.^{10c} We further disclosed that the alcohol-pendant *N*-hydroxyethyl on [12]aneN₃ and cyclen formed 1:1 Zn^{II} complexes **7**¹³ and **8**,¹⁴ which more efficiently catalyze 4-nitrophenyl acetate hydrolysis. These were the novel models of metalocatalysts that *indirectly* hydrolyze the carboxyl ester via the rate-limiting "acyl intermediates" **9** and **10**, respectively. Using **8** and bis(4-nitrophenyl) phosphate



(BNP⁻), we also checked the phosphatase activity in aqueous solution. The phosphoryl transfer reaction from BNP⁻ to **8** could be followed as 4-nitrophenolate production,¹⁵ but the following reaction was too complex to allow the elucidation of the total reaction mechanism.

In this study, we synthesized a new benzyl alcohol-pendant cyclen **11**, bearing a chiral carbon adjacent to the phenyl group. We have discovered that **11** yields a 1:1 Zn^{II} complex whose phosphoester bond cleavage activity has a very distinct reaction mechanism. We herein describe a novel chemical model for Zn^{II}-involving serine enzymes as part of our series of studies on the intrinsic chemical properties of Zn^{II} in alkaline phosphatase. We also attempted the enantioselective hydrolysis of various carboxyesters with **11**, which will be reported elsewhere.



(11) (a) Kimura, E.; Koike, T. *Comments Inorg. Chem.* **1991**, *11*, 285-301. (b) Kimura, E. In *Progress in Inorganic Chemistry*; Karlin, K. D., Ed.; John Wiley & Sons: New York, 1994; Vol. 41, 443-492.

(12) Koike, T.; Takamura, M.; Kimura, E. *J. Am. Chem. Soc.* **1994**, *116*, 8443-8449.

(13) Kimura, E.; Nakamura, I.; Koike, T.; Shionoya, M.; Kodama, Y.; Ikeda, T.; Shiro, M. *J. Am. Chem. Soc.* **1994**, *116*, 4764-4771.

(14) Koike, T.; Kajitani, S.; Nakamura, I.; Kimura, E.; Shiro, M. *J. Am. Chem. Soc.* **1995**, *117*, 1210-1219.

(15) The second-order rate constant for the 4-nitrophenolate release reaction from BNP⁻ with **8** (determined by initial slope method) is (5.0 ± 0.1) × 10⁻⁴ M⁻¹ s⁻¹ in aqueous solution at 35 °C with *l* = 0.10 (NaNO₃). Kimura, E.; Koike, T. Unpublished results.

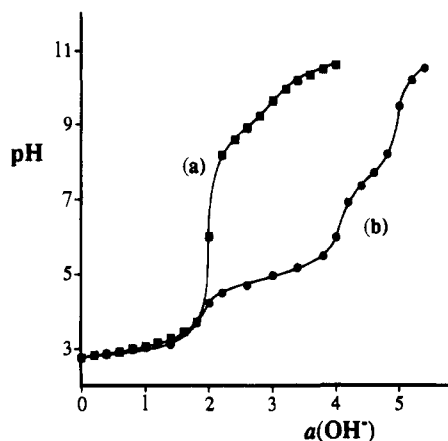
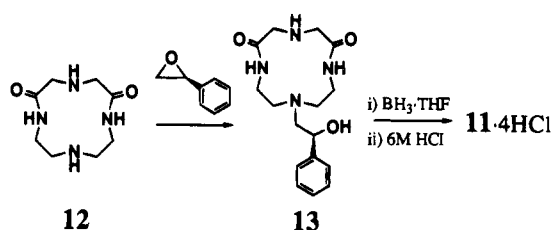


Figure 1. Typical titration curves for **11** at 25 °C with $I = 0.10$ (NaClO_4): (a) 1.0 mM of **11**·4HCl; (b) a + 1.0 mM ZnSO_4 .

Scheme 2



Results and Discussion

Synthesis of (S)-1-(2-Hydroxy-2-phenylethyl)-1,4,7,10-tetraazacyclododecane (Benzyl Alcohol-Pendant Cyclen, **11) (Scheme 2).** The macrocyclic dioxotetraamine **12**¹⁶ and (*S*)-styrene oxide were heated to reflux in EtOH for 1 day to obtain (*S*)-1-(2-hydroxy-2-phenylethyl)-5,9-dioxo-1,4,7,10-tetraazacyclododecane (**13**) in 46% yield. Both amide groups were reduced with BH_3 -THF complex in THF to give (*S*)-1-(2-hydroxy-2-phenylethyl)-1,4,7,10-tetraazacyclododecane (**11**), which was isolated as its tetrahydrochloride salt from 6 M HCl aqueous solution in 62% yield. Using *rac*-styrene oxide as the starting material, the corresponding racemic ligand was yielded in 24%. For all the following studies, we used the enantiomeric product **11**.

Protonation and Zinc(II) Complexation Constants of the Benzyl Alcohol-Pendant Cyclen (11**).** The protonation constants (K_n) of **11** were determined by potentiometric pH titrations of **11**·4HCl (1 mM) using 0.10 M NaOH with $I = 0.10$ (NaClO_4) at 25 °C. A typical pH titration curve is shown in Figure 1a. The titration data were analyzed for equilibria 1–4. The mixed protonation constants K_1 – K_4 (a_{H^+} is the activity of H^+) are defined as follows:

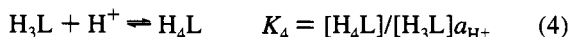
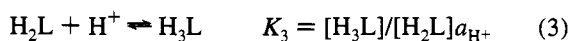
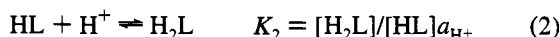
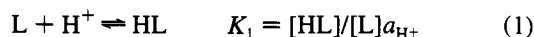


Table 1 summarizes the obtained protonation constants ($\log K_n$) in comparison with the reported K_n values of cyclen and *N*-(hydroxyethyl)cyclen (HE-cyclen) under the same conditions. The K_1 and K_2 values of **11** are extremely large with respect to

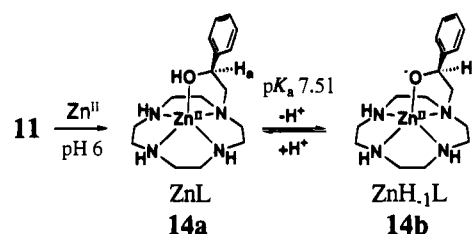
(16) Kimura, E.; Kuramoto, Y.; Koike, T.; Fujioka, H.; Kodama, M. *J. Org. Chem.* **1990**, *55*, 42–46.

Table 1. Comparison of the Protonation Constants of Cyclen Ligands and Zn^{II} Complexation Constants^a

	11	cyclen	HE-cyclen	methylcyclen
$\log K_1$	10.92 ± 0.05^b	11.04^c	10.72^c	
$\log K_2$	8.87 ± 0.03^b	9.86^c	9.28^c	
$\log K_3$	$<2^b$	$<2^c$	$<2^c$	
$\log K_4$	$<2^b$	$<2^c$	$<2^c$	
$\log K(\text{ZnL})$	13.6 ± 0.1^d	15.3^c	13.8^c	15.1^e
$\text{p}K_a$				
25 °C	7.51 ± 0.02^f	7.86^g	7.60^h	7.68^e
35 °C	7.30 ± 0.02^i	7.64^g	7.41^h	7.50 ± 0.02^j

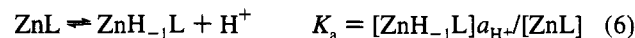
^a $K_n = [\text{H}_n\text{L}]/[\text{H}_{n-1}\text{L}]a_{\text{H}^+}$. $K(\text{ZnL}) = [\text{ZnL}]/[\text{L}][\text{Zn}^{\text{II}}]$. $\text{p}K_a = -\log([\text{ZnH}_{-1}\text{L}]/[\text{ZnL}])$. ^b At 25 °C with $I = 0.10$ (NaClO_4). ^c From ref 14 at 25 °C with $I = 0.10$ (NaClO_4). ^d Determined with 1.0 mM of **14a** and 4 equiv of HClO_4 at 25 °C with $I = 0.10$ (NaClO_4). ^e From ref 17 at 25 °C with $I = 0.10$ (NaClO_4). ^f From ref 12 with $I = 0.10$ (NaClO_4). ^g From ref 14 with $I = 0.10$ (NaClO_4). ^h Determined with 1.0 mM of **14a** and $I = 0.10$ (NaNO_3). ⁱ Determined with 1.0 mM of **15a** and $I = 0.10$ (NaNO_3).

Scheme 3

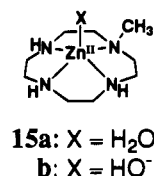


K_3 and K_4 values, which are roughly the same as those of cyclen and HE-cyclen.

The potentiometric pH titration curve of **11**·4HCl in the presence of an equimolar amount of Zn^{II} using 0.10 M NaOH (Figure 1b) revealed two distinct equilibria: the first is the ZnL complex formation at $4 < \text{pH} < 6$ until $a = 4$, and the second is monodeprotonation from ZnL ($4 < a < 5$). Up to $a = 4$, the equilibration was extremely slow, so that we had to wait more than 2 h for each titration point. The titration data were treated for the 1:1 ZnL (**14a**) complex (eq 5) and its monodeprotonated complex ZnH_{-1}L (**14b**) (eq 6),



where H_{-1}L denotes alcoholic OH-deprotonated ligand (Scheme 3). The obtained values $\log K(\text{ZnL})$ at 25 °C and deprotonation constants $\text{p}K_a$ at 25 and 35 °C and listed in Table 1. Any further deprotonation or precipitation of $\text{Zn}(\text{OH})_2$ was not observed over pH 12, indicating the monodeprotonated species to be stable until pH ca. 12. The deprotonation constants $\text{p}K_a$ (eq 6) of 7.51 ± 0.02 and 7.30 ± 0.02 determined by the pH-metric titration respectively at 25 °C with $I = 0.10$ (NaClO_4) and 35 °C with $I = 0.10$ (NaNO_3) are near those of **6a**¹² and Zn^{II} -*N*-methylcyclen **15a**¹⁷(see Table 1). Fortunately, both the ZnL



(**14a**) and ZnH_{-1}L (**14b**) complexes were crystallized as their

(17) Shionoya, M.; Ikeda, T.; Kimura, E.; Shiro, M. *J. Am. Chem. Soc.* **1994**, *116*, 3848–3859. The Zn^{II} complexation constant $\log K(\text{ZnL})$ for **15a** is 15.1 ± 0.1 at 25 °C with $I = 0.10$ (NaClO_4). Kimura, E.; Ikeda, T. Unpublished results.

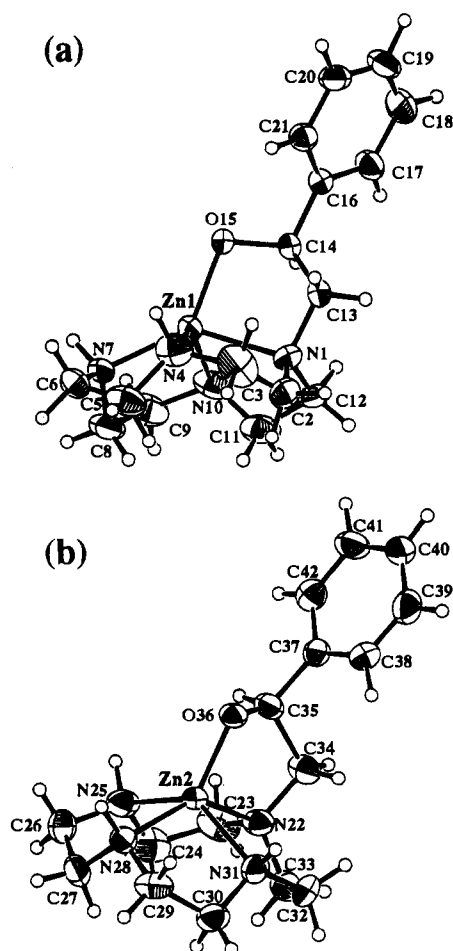


Figure 2. ORTEP drawing (30% probability ellipsoids) of the two crystallographically distinct molecules (a and b) of **14b**·ClO₄. ClO₄ anions were omitted for clarity. Bond distances: (a) Zn(1)–O(15) 1.915(5), Zn(1)–N(1) 2.172(7), Zn(1)–N(4) 2.173(8), Zn(1)–N(7) 2.067(7), Zn(1)–N(10) 2.143(8) Å; (b) Zn(2)–N(22) 2.155(7), Zn(2)–N(25) 2.161(8), Zn(2)–N(28) 2.056(7), Zn(2)–N(31) 2.169(7) Å. Bond angles: (a) N(1)–Zn(1)–N(4) 81.2(3), N(1)–Zn(1)–N(10) 81.4(4), N(4)–Zn(1)–N(7) 84.0(4), N(7)–Zn(1)–N(10) 82.2(4), O(15)–Zn(1)–N(1) 86.8(2)°; (b) N(22)–Zn(2)–N(25) 82.8(4), N(22)–Zn(2)–N(31) 80.6(3), N(25)–Zn(2)–N(28) 82.1(3), N(28)–Zn(2)–N(31) 82.8(3), O(36)–Zn(2)–N(22) 86.7(2)°.

perchlorate salts from pH 6 and 9.5 aqueous solutions, respectively. The structure of the monodeprotonated complex **14b** was confirmed by the X-ray crystal analysis (vide infra). As the solution pH became higher, the chemical shifts of the benzyl proton H_a for **14** moved upfield from δ 5.14 at pD 6.0 (**14a**) to δ 4.86 at pD > 9.5 (**14b**). From these facts and the following results, we assigned the deprotonated structure to be **14b** rather than Zn^{II}–OH[–] species in aqueous alkaline solution.

X-ray Crystal Structure of the Zn^{II} Complex of the Deprotonated Benzyl Alcohol-Pendant Cyclen (14b**).** When the benzyl alcohol-pendant cyclen **11** (in the acid-free form L, see the Experimental Section) in water was mixed with 1 equiv of Zn^{II}(ClO₄)₂·6H₂O at 60 °C, **14a**·(ClO₄)₂ was obtained as colorless crystals. Addition of 1 equiv of NaOMe to **14a**·(ClO₄)₂ in MeOH gave **14b**·ClO₄, which was recrystallized from aqueous alkaline solution (pH 9.5).

Figure 2 shows an ORTEP drawing of **14b**·ClO₄ with 30% probability thermal ellipsoids. Selected crystal data and collection parameters are displayed in Table 2. In this Zn^{II} complex, there are two crystallographically distinct molecules (Figure 2a,b). The Zn^{II} ions Zn1 and Zn2, respectively, lie above the four nitrogen atoms (N₁, N₄, N₇, N₁₀ and N₂₂, N₂₅, N₂₈, N₃₁), and are apically bound with the pendant alkoxide oxygens O₁₅ and O₃₆, respectively. The angles N₁–Zn₁–N₇ and N₂₂–

Table 2. Selected Crystallographic Data for **14b**·ClO₄

empirical formula	C ₁₆ H ₂₇ N ₄ O ₅ ClZn
formula weight	456.25
crystal color, habit	colorless, prismatic
crystal system	orthorhombic
space group	P2 ₁ 2 ₁ 2 ₁ (no. 19)
lattice parameters	<i>a</i> = 16.977(4) Å <i>b</i> = 18.135(4) Å <i>c</i> = 13.173(3) Å <i>V</i> = 4055(1) Å ³ <i>Z</i> = 8
μ (Cu K α)	31.96 cm ^{–1}
radiation	Cu K α (λ = 1.541 78 Å) graphite monochromated
scan type	ω –2 θ
scan rate (in ω)	16.0 deg/min (five scans)
scan width	(1.42 + 0.30 tan θ)
2 θ _{max}	120.2
no. of reflns measd	3414 (total)
refinement	full-matrix least squares
no. of obs (<i>I</i> > 3.00 σ (<i>I</i>))	2862
residuals: <i>R</i> ; <i>R</i> _w	0.050; 0.077

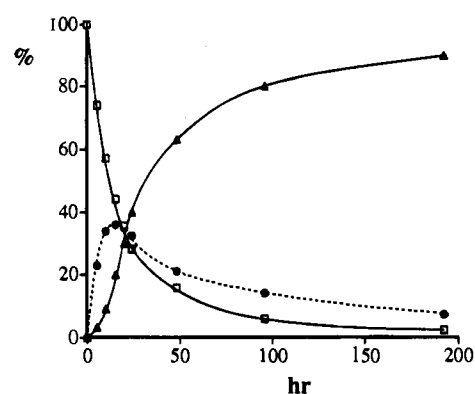


Figure 3. Time course of the relative concentrations of Zn^{II} complexes **14b** (open square), **16** (solid circle), and **17** (solid trigone) for the reaction of BNP[–] (25 mM) with **14b** (20 mM) in D₂O at 35 °C, *I* = 0.10 (NaNO₃), and pD = 10.3 (0.1 M CHES buffer). The relative concentrations (%) are based on the initial concentration of **14b**.

Zn₂–N₂₈ and N₄–Zn₁–N₁₀ and N₂₅–Zn₂–N₃₁ are respectively bent at 138.5 and 139.2° and 135.0 and 134.5°, indicating distorted tetragonal-pyramidal structures. The average Zn–O[–] bond distance of 1.91 Å is much shorter than the Zn–N bonds (2.056–2.173 Å). The Zn–O[–] distance is shorter in the Zn^{II}–anion donor than in other Zn^{II}–macrocyclic polyamine complexes.^{10b,13,14,18} The earlier Zn–O bond distance with the neutral alcohol pendant in **8** was 1.994 Å.¹⁴ The apical Zn–O[–] bond is bent with the N₁–Zn₁–O₁₅ and N₂₂–Zn₂–O₃₆ angles of 86.8 and 86.7°, respectively. One may view **14b** as having a distorted trigonal-bipyramidal structure with N₁, N₇, and O₁₅ as equatorial donors and N₄ and N₁₀ as axial donors.

Although the pendant alkoxide donor binds firmly with Zn^{II} in the solid state, this bonding would be kinetically labile in DMF and H₂O solutions, so that this alkoxide anion can be a good nucleophile for the phosphoryl transfer reaction with BNP[–].

Net Reaction of the Benzyl Alcohol-Pendant Cyclen–Zn^{II} Complex **14b with Bis(4-nitrophenyl) Phosphate (BNP[–]).** The ZnH_{–1}L complex **14b** has been tested as a simplified model of AP. Since the phosphomonoester (e.g., 4-nitrophenyl phosphate (NPP^{2–})) was hydrolyzed impractically slowly, we used a more reactive substrate, phosphodiester bis(4-nitrophenyl) phosphate (BNP[–]).

The overall reaction of BNP[–] (25 mM) with **14b** (20 mM) was followed by the ¹H NMR of the benzyl protons in D₂O at 35 °C and pD = 10.3 (0.1 M CHES buffer) (see Figure 3). The

(18) Kimura, E.; Koike, T.; Toriumi, K. *Inorg. Chem.* **1988**, *27*, 3687–3688.

Scheme 4

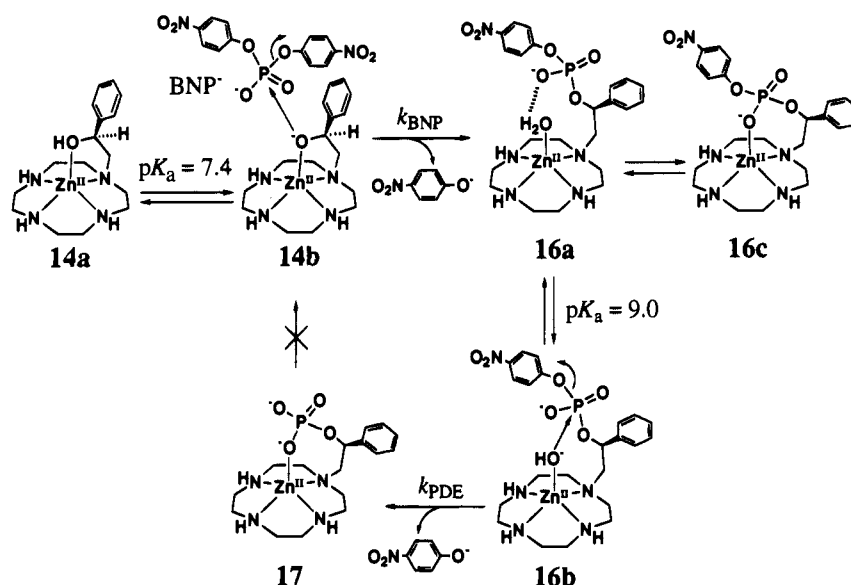


Table 3. Comparison of the Phosphodiester Bond Cleavage Rate Constants, k_{BNP} ($\text{M}^{-1} \text{s}^{-1}$), for **14b**, **8**, **15b**, **5b**, and **6b**, and Aqueous OH^- Ion in Aqueous Solution

catalyst	k_{BNP}	catalyst	k_{BNP}
14b	$(6.5 \pm 0.1) \times 10^{-4}{}^a$	5b	$8.5 \times 10^{-5}{}^b$
8	$5.0 \times 10^{-4}{}^c$	6b	$2.1 \times 10^{-5}{}^b$
15b	$(5.2 \pm 0.2) \times 10^{-6}{}^d$	OH^- (aq)	$2.4 \times 10^{-5}{}^b$

^a Determined with 2.0, 1.0, and 0.5 mM **14b** and 10, 5.0, and 2.5 mM BNP^- at 35 °C with $I = 0.10$ (NaNO_3). ^b From ref 10c at 35 °C with $I = 0.20$ (NaClO_4). ^c From ref 15 at 35 °C with $I = 0.10$ (NaNO_3). ^d Determined with 16, 8.0, and 4.0 mM **14b** and 10, 5.0, and 2.5 mM BNP^- at 35 °C with $I = 0.10$ (NaNO_3).

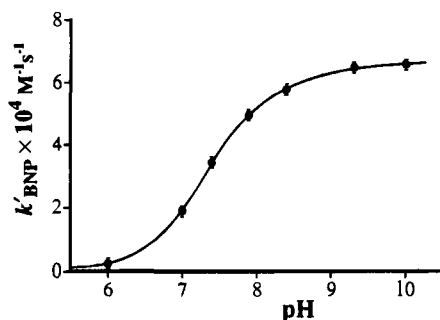


Figure 4. Rate-pH profile for the second-order rate constants of the phosphoryl transfer from BNP^- to **14** (see eq 7) at 35 °C with $I = 0.10$ (NaNO_3) in aqueous solution.

initial product **16** (a new triplet at δ 5.56), which later was proven to be the phosphoryl intermediate, increased as the starting **14b** (δ 4.83) decreased. The final product **17** (δ 5.90, see blow) appeared subsequently. After 192 h, **14b** and **16** diminished to 2.5% and 7.5%, respectively, and the majority (90%) of the initial Zn^{II} complex was converted to **17**, where almost 2 equiv of 4-nitrophenolate was released (191% based on initial concentration of **14b**). The same reaction was followed by ^{31}P NMR under the same conditions, and the products **16** and **17** were identified as δ -5.7 and 5.9, respectively. No other side product was detected. We assigned the net reaction scheme as depicted in Scheme 4, with the aid of the following results.

A Kinetic Study of the Initial Reaction $14b \rightarrow 16$. The initial phosphorylation rate in aqueous solution at 35 °C, $I = 0.10$ (NaNO_3), and pH 6.0–10.3 (20 mM Good's buffer) was followed by the appearance of 4-nitrophenolate at 400 nm. The second-order dependence of the rate constant k'_{BNP} on the total

concentration of Zn^{II} complex ($= [\mathbf{14a}] + [\mathbf{14b}]$) and $[\text{BNP}^-]$ fits the kinetic eq 7, where ν is the 4-nitrophenolate releasing rate. The second-order rate constant, k'_{BNP} is plotted as a function of pH (see Figure 4). The resulting sigmoidal curve indicates a kinetic process controlled by an acid–base equilibrium. The inflection point at pH 7.4 is almost the same as the $\text{p}K_{\text{a}}$ value of **14** for the pendant alcohol deprotonation (eq 6). Therefore, the reactive species is concluded to be the deprotonated complex **14b**. The second-order rate constant k_{BNP} (see eq 8) of $(6.5 \pm 0.1) \times 10^{-4} \text{M}^{-1} \text{s}^{-1}$ was determined from the maximum k'_{BNP} values.

$$\nu = k'_{\text{BNP}}[\text{total Zn}^{\text{II}} \text{ complex}][\text{BNP}^-] \quad (7)$$

$$= k_{\text{BNP}}[\mathbf{14b}][\text{BNP}^-] \quad (8)$$

For a reference, the hydrolysis of the same substrate BNP^- (to NPP^{2-}) with Zn^{II} -*N*-methylcyclohexyl **15** has been determined by the same method. The kinetics followed the second-order dependence on $[\text{BNP}^-]$ and $[\mathbf{15b}]$. The rate constant is $(5.2 \pm 0.2) \times 10^{-6} \text{M}^{-1} \text{s}^{-1}$ at 35 °C, $I = 0.10$ (NaNO_3), and pH 9.3 (20 mM CHES buffer), which demonstrates that the nucleophilic reaction catalyzed by **14b** is 125 times faster than by **15b**. It is understood that the Zn^{II} -alkoxide anion is a better nucleophile than Zn^{II} -hydroxide anion toward the phosphate substrate, just as toward 4-nitrophenyl acetate substrate.^{13,14} It should be noted, however, that the reaction with Zn^{II} -alkoxide **14b** is a phosphoryl transfer to form a phosphoryl intermediate **16b** (see Scheme 4), as the previously found acyl transfer with **7** and **8**.^{13,14} On the other hand, the reaction with **15b** is a hydrolysis that yields NPP^{2-} .

Isolation of the Phosphoryl Intermediate **16a from the BNP^- Reaction with **14b** in DMF.** The phosphoryl intermediate **16a** was unequivocally determined by independent isolation of $\mathbf{16a}\text{-ClO}_4$ by the reaction of BNP^- and **14b** in dry DMF. The structure was identified by elemental analysis (C, H, N) and ^1H , ^{13}C , and ^{31}P NMR. The pH-metric titration of **16a** at 35 °C with $I = 0.10$ (NaNO_3) using 0.1 M aqueous NaOH ¹⁹ showed the monodeprotonation and its $\text{p}K_{\text{a}}$ of 9.10 ± 0.05 , which is assigned to $\mathbf{16a} \rightleftharpoons \mathbf{16b}$. The $\text{p}K_{\text{a}}$ value is higher than 7.50 ± 0.02 for $\mathbf{15a} \rightleftharpoons \mathbf{15b}$ at the same conditions, which is possibly due to the proximate phosphate anion binding to the

(19) Hence, the $\text{p}K_{\text{a}}$ was determined using the titration data before 0.5% hydrolysis of pendant phosphate.

Zn^{II}, see **16c**. The ³¹P NMR chemical shift of phosphoryl intermediate **16** in D₂O changed from δ -3.6 at pD 6.5 (**16a**) to δ -6.5 at pD 11 (**16b**).

The reaction of BNP⁻ with **14b** (the isolated monoperchlorate salt was used) in dry DMF at 35 °C was kinetically studied by observing the appearance of 4-nitrophenolate at 430 nm. The second-order rate constant k_{BNP} ($= 1.1 \pm 0.1 \text{ M}^{-1} \text{ s}^{-1}$) with respect to [BNP⁻] and [**14b**] was obtained. The comparison of the rate constants k_{BNP} in DMF and aqueous solution points out that the Zn^{II}-bound alkoxide nucleophile acts 1700 times more efficiently in this aprotic solvent than in aqueous solution, which is accounted for by less interfering solvations in DMF.²⁰ This observation suggests that in hydrophobic environments a phosphoryl transfer at the enzyme active center might occur quite effectively.

Spontaneous Hydrolysis of the Pendant Phosphodiester in 16b to a Phosphomonoester 17 by the Intramolecular Zn^{II}-OH⁻. The pendant phosphodiester in **16**, the initial phosphorylation product resulting from the phosphotransfer reaction, was found to undergo spontaneous hydrolysis in alkaline aqueous solution to yield a phosphomonoester **17** (see Scheme 4). We failed to isolate **17** as a solid. This reaction was followed by the ¹H and ³¹P NMR spectral changes. The disappearance of the reactant **16** (5 mM) (δ 5.56 (OCHC), 6.85 and 8.03 (O₂NArH) for ¹H; δ -5.7 for ³¹P) matched the appearance of the product **17** (δ 5.09 (OCHC) for ¹H; δ 5.9 for ³¹P) and 4-nitrophenolate (δ 6.53 and 8.06) in D₂O at 35 °C and pD = 10.3 (0.1 M CHES buffer).

The hydrolysis rate (ν_2) of the phosphodiester pendant in **16** was followed by UV spectroscopic measurement (at 400 nm) at pH 7.0–10.5 (20 mM Good's buffer), $I = 0.10$ (NaNO₃), and 35 °C. The first-order dependence on the total concentration of **16** ($= [\mathbf{16a}] + [\mathbf{16b}] + [\mathbf{16c}]$) is consistent with the kinetic eq 9. The first-order rate constants k'_{PDE} are plotted as a function of pH in Figure 5. The sigmoidal curve indicates characteristic of a kinetic process controlled by an acid–base equilibrium and exhibits an inflection point at pH 9.0, which is almost the same as the pK_a value of 9.1 for the coordinate water of **16a**. Therefore, just as all the previous Zn^{II}-OH⁻ species,^{9d,10c} the Zn^{II}-OH⁻ in **16b** must be a good nucleophile to the intramolecular phosphate. The first-order rate constant k_{PDE} of $(3.5 \pm 0.1) \times 10^{-5} \text{ s}^{-1}$ was obtained from the maximum k'_{PDE} (eq 10).

$$\nu_2 = k'_{\text{PDE}}[\text{total ZnL complex } \mathbf{16}] \quad (9)$$

$$= k_{\text{PDE}}[\mathbf{16b}] \quad (10)$$

A prolonged (ca. 1 week) alkaline reaction at 35 °C in 0.1 M aqueous NaOD solution did not change the ³¹P NMR of **17** (δ 5.9), indicating that **17** is inert and undergoes no more hydrolysis. We assign the final product to the intramolecular phosphomonoester coordinating structure **17**. Earlier, we found that the Zn^{II}-cyclen complex **6a** tends to strongly bind to dianionic phosphomonoester, e.g., $\log K = 3.3$ for 1:1 the NPP²⁻-Zn^{II}-cyclen complex.¹⁴ Treatment of **17** (5 mM)²¹ with EDTA (25 mM) in D₂O at pD 10.3 (0.1 M CHES buffer) stripped Zn^{II} to free the ligand showing a singlet ³¹P signal at δ 4.2.

(20) (a) A second-order rate constant for hydrolysis of 4-nitrophenyl acetate with **14b** in DMF ($(1.1 \pm 0.1) \times 10^2 \text{ M}^{-1} \text{ s}^{-1}$ at 35 °C) is also 350 times greater than the rate in aqueous solution ($0.31 \pm 0.01 \text{ M}^{-1} \text{ s}^{-1}$ at 35 °C with $I = 0.10$ (NaNO₃)). Kimura, E.; Kodama, Y. Unpublished results. (b) We have given a thought to running the hydrolysis with Zn^{II}-OH⁻ complex **15b** in dry DMF as a reference reaction. However, we could not isolate **15b** in any of the attempts using various counteranions such as ClO₄⁻, PF₆⁻, Cl⁻, etc. Generation of **15b** in situ makes the reaction more complex and difficult to interpret.

(21) The solution of **17** was prepared by the reaction of **16a** (5 mM) in D₂O at 50 °C and pD 10.3 (0.1 M CHES buffer) for 1 day.

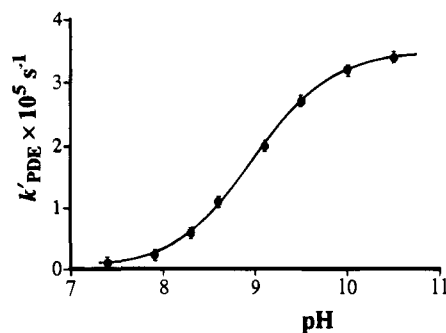
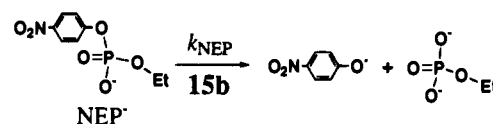
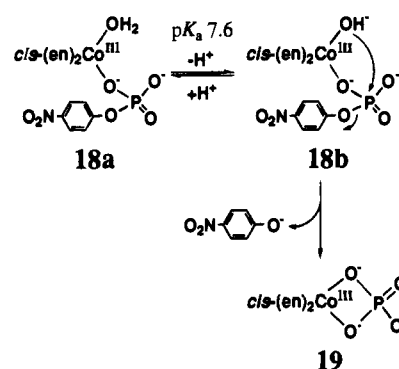


Figure 5. Rate–pH profile for the first-order rate constants of intramolecular phosphodiester hydrolysis of **16** (see eq 9) at 35 °C with $I = 0.10$ (NaNO₃) in aqueous solution.

Scheme 5



Scheme 6



Hydrolysis of Ethyl 4-Nitrophenyl Phosphate (NEP⁻) with an Intermolecular Nucleophile Zn^{II}-OH⁻ **15b (Scheme 5). A Reference Reaction to the Intramolecular Hydrolysis of **16b**.** In order to see the efficiency of the intramolecular attack of Zn^{II}-OH⁻ at the pendant phosphodiester in **16b** → **17**, we have measured the rate of an intermolecular reaction between ethyl 4-nitrophenyl phosphate (NEP⁻) and (*N*-methylcyclen)-Zn^{II}-OH⁻ (**15b**) (Scheme 5) under the same conditions. The kinetics, followed by the appearance of 4-nitrophenolate at pH 9.3, showed the second-order rate constant k_{NEP} of $(7.9 \pm 0.3) \times 10^{-7} \text{ M}^{-1} \text{ s}^{-1}$. One can calculate the effective molarity of 45 M ($= k_{\text{PDE}}/k_{\text{NEP}}$) for the intramolecular phosphate of **16b**. In other words, the hydrolysis by the intramolecular Zn^{II}-OH⁻ (**16b**) is 45 000 times faster than by the intermolecular Zn^{II}-OH⁻ (1 mM **15b**).

The hydrolysis of the phosphoryl intermediate **16** by the intramolecular Zn^{II}-OH⁻ nucleophile is somewhat analogous to the Lindoy and Sargeson's Co^{III} model system (Scheme 6).^{9b} The sigmoidal pH dependence of the hydrolysis rate (pH 6–9) implies the **18a** ⇌ **18b** equilibrium with pK_a of 7.6, and the intramolecular Co^{III}-OH⁻ nucleophile efficiently attacks the Co^{III}-bound monophosphate with the first-order rate constant of $7.8 \times 10^{-4} \text{ s}^{-1}$ to form the product **19**.

Summary and Conclusions

The two-step mechanism of phosphate ester hydrolysis by Zn^{II}-containing alkaline phosphatase (AP) (Scheme 1) is well mimicked by the newly designed complex **14**: (i) a phosphoryl intermediate **16** is generated by attack of the hydroxy moiety of the alcohol pendant at the BNP⁻ (one of the ester group is

concomitantly hydrolyzed) and (ii) the phosphoryl intermediate **16** is hydrolyzed by the intramolecular $Zn^{II}-OH^-$. The attack at the BNP^- substrate and hydrolysis of the intermediate both require Zn^{II} . For the first step, the hydroxyl group is activated by Zn^{II} at physiological pH to **14b** ($pK_a = 7.4$), which is a 125 times more effective nucleophile to the phosphate substrate than the Zn^{II} -activated water of the reference **15b**. For the second step, the intramolecular nucleophile is generated from $Zn^{II}-OH_2$ **16a** with a pK_a value of 9. This intramolecular hydrolysis is 45 000 times faster than the intermolecular hydrolysis of NEP^- with 1 mM **15b**. In the AP enzyme (Scheme 1), these two functions of Zn^{II} are performed separately by two proximate Zn^{II} atoms; one is involved in the activation of Ser-102 to yield phosphoryl intermediate **2**, and the other is involved in the activation of H_2O **3** to attack the intermediate **2**. The intramolecular arrangement of these two Zn^{II} ions in AP is more advantageous than our single- Zn^{II} system in order to provide this dual role, wherein the pK_a value of 9.0 (due to the close phosphate anion or the phosphate-binding) for **16a** \rightleftharpoons **16b** is higher than the reported pK_a value of 7.4 for **2** \rightleftharpoons **3** in the enzyme.

Scheme 4 summarizes the whole reaction mechanism of the P-O bond cleavage of the phosphodiester (BNP^-) by **14**. The final phosphomonoester product **17**, unfortunately, was found to be very inert under normal conditions (all the attempts to hydrolyze it failed, including raising the pH as high as 11). Therefore, we could not use **14** as a catalyst. However, the present results may well serve the novel elucidation of the collaborative roles of Ser-102 and Zn^{II} in alkaline phosphatase.

Experimental Section

General Information. All reagents and solvents used were of analytical grade. The Good's buffers (Dojindo) were commercially available and used without further purification: MES (2-(*N*-morpholino)ethanesulfonic acid, $pK_a = 6.2$), MOPS (3-(*N*-morpholino)propanesulfonic acid, $pK_a = 7.2$), HEPES (*N*-(2-hydroxyethyl)piperazine-*N'*-2-ethanesulfonic acid, $pK_a = 7.6$), EPPS (*N*-(2-hydroxyethyl)piperazine-*N'*-3-propanesulfonic acid, $pK_a = 8.0$), TAPS ((*N*-(tris(hydroxymethyl)methyl)amino)-3-propanesulfonic acid, $pK_a = 8.4$), CHES (2-(cyclohexylamino)ethanesulfonic acid, $pK_a = 9.5$), CAPSO (3-(*N*-cyclohexylamino)-2-hydroxypropanesulfonic acid, $pK_a = 10.0$), CAPS (3-(*N*-cyclohexylamino)propanesulfonic acid, $pK_a = 10.4$). Sodium bis-(4-nitrophenyl) phosphate was crystallized from an aqueous solution of bis(4-nitrophenyl) phosphoric acid (BNP) and equimolar NaOH. Lithium ethyl 4-nitrophenyl phosphate was prepared by the reported method.²² DMF was distilled in vacuo over anhydrous $MgSO_4$ and stored in the dark. All aqueous solutions were prepared using deionized and distilled water.

Kinetic study was carried out using a Hitachi U-3500 spectrophotometer equipped with a thermoelectric cell temperature controller (± 0.5 °C). IR spectra were recorded on a Shimadzu FTIR-4200. 1H (400 MHz), ^{13}C (100 MHz), and ^{31}P (162 MHz) NMR spectra were recorded on a JEOL α -400 spectrometer. 3-(Trimethylsilyl)propionic-2,2,3,3-*d*₄ acid sodium salt (Aldrich) in D_2O and tetramethylsilane (Merck) in organic square were used as internal references for 1H and ^{13}C NMR measurements. A D_2O solution of 80% phosphoric acid was used as an external reference for ^{31}P NMR measurement. Optical rotations were recorded on a Union Giken Automatic Digital Polarimeter PM-101 at 22.0 ± 0.5 °C. Melting points were determined by using a Yanaco micro melting apparatus without any corrections. Elemental analysis was performed on a Yanaco CHN Corder MT-3. Thin layer (TLC) and silica gel column chromatographies were carried out on Merck Art. 5554 (silica gel) TLC plates and Wakogel C-300 (silica gel), respectively.

Synthesis of (S)-1-(2-Hydroxy-2-phenylethyl)-1,4,7,10-tetraazacyclododecane (11). 2,6-Dioxo-1,4,7,10-tetraazacyclododecane (**12**) (2.00 g, 10 mmol)¹⁶ and (S)-styrene oxide (1.32 g, 11 mmol) were

heated to reflux in EtOH (100 mL) for 1 day. The reaction mixture was evaporated to dryness. The residue was purified by silica gel column chromatography (eluent $CH_2Cl_2/MeOH/28\%$ aqueous $NH_3 = 40:3:0.1$) followed by crystallization from CH_3CN to yield 1-(2-hydroxy-2-phenylethyl)-5,9-dioxo-1,4,7,10-tetraazacyclododecane (**13**) as colorless prisms (1.47 g, 4.6 mmol, 46% yield): mp 192.0–193.0 °C; IR (KBr pellet) 3362, 3086, 2975, 2955, 2822, 1655, 1539, 1455, 1435, 1348, 1316, 1291, 1269, 1227, 1200, 1169, 1071, 920, 870, 843, 774, 758, 706 cm^{-1} ; TLC (eluent $CH_2Cl_2/MeOH/28\%$ aqueous $NH_3 = 5:1:0.2$) $R_f = 0.4$; 1H NMR ($CDCl_3$) δ 1.83–2.06 (1H, br, amine NH), 2.51 (2H, dt, $J = 13.2, 4.6$ Hz, NCH), 2.64 (1H, dd, $J = 13.2, 4.6$ Hz, NCH), 2.64 (1H, dd, $J = 13.6, 4.0$ Hz, NCHCPh), 2.77 (2H, ddd, $J = 13.2, 9.0, 4.2$ Hz, NCH), 2.84 (1H, dd, $J = 13.6, 9.4$ Hz, NCHCPh), 3.16–3.24 (1H, br, alcohol OH; 2H, m, CONCH), 3.29 (1H, d, $J = 16.2$ Hz, CHCON), 3.34 (1H, d, $J = 16.2$ Hz, NCOCH), 3.41–3.48 (2H, m, CONCH), 4.79 (1H, dd, $J = 9.4, 4.0$ Hz, CHPh), 7.30 (1H, t, $J = 6.4, 2.0$ Hz, Ph), 7.35–7.42 (4H, m, Ph), 7.43–7.48 (2H, br, amide NH); $[\alpha]_D -55.9^\circ$ (c 1.00, MeOH).

To a suspended solution of dioxo macrocycle **13** (1.92 g, 6.0 mmol) in dry THF (40 mL) was added slowly a THF solution (65 mL) of 1 M BH_3-THF complex at 0 °C. The mixture was stirred at room temperature for 1 h and then heated at 60 °C for 1 day. After decomposition of the excess amount of the hydroborane complex with water at 0 °C, the solvent was evaporated. The residue was dissolved in 6 M aqueous HCl (70 mL) and then the solution was heated at 70 °C for 2 h. The mixture was washed with CH_2Cl_2 (30 mL \times 2) and evaporated to dryness. The residue was passed through an anion exchange column of Amberlite IRA-400 with water to obtain **11** as a colorless oil. Crystallization of the oil from 6 M aqueous HCl afforded colorless needles as its tetrahydrochloride salt ($11 \cdot 4HCl$) in 62% yield (1.63 g, 3.7 mmol): dec 210°; IR (KBr pellet) 3420, 2998, 2793, 2448, 1576, 1495, 1439, 1066, 1028, 766, 704 cm^{-1} ; 1H NMR (D_2O , pD 1.0) δ 2.82–3.21 (18H, m, NCH_2), 4.89 (1H, t, $J = 6.2$, OCHC), 7.40–7.54 (5H, m, ArH); ^{13}C NMR (D_2O , pD 1.0) δ 41.4, 41.5, 44.5, 44.6, 45.4, 47.0, 52.3, 52.4, 62.0, 73.8, 129.0, 131.5, 132.2, 144.8; $[\alpha]_D -49.1^\circ$ (c 1.00, H_2O). Anal. Calcd for $C_{16}H_{32}N_4OCl_4 \cdot \frac{1}{2}H_2O$: C, 43.0; H, 7.44; N, 12.5. Found: C, 43.1; H, 7.49; N, 12.4.

Synthesis of (S)-1-(2-Hydroxy-2-phenylethyl)-1,4,7,10-tetraazacyclododecane-Zinc(II) Complex ($14a \cdot (ClO_4)_2$). $11 \cdot 4HCl$ (438 mg, 1.0 mmol) was passed through an anion exchange column of Amberlite IRA-400 with water to obtain the free ligand **11** as a colorless oil. After the oil was dissolved in water (4 mL), $Zn(ClO_4)_2 \cdot 6H_2O$ (391 mg, 1.1 mmol) was added in the solution. The solution was stirred at 60 °C for 1 h. After the solvent was evaporated, the residue was recrystallized from water to obtain colorless prisms as diperchlorate salts $14a \cdot (ClO_4)_2$ in 91% yield (507 mg, 0.91 mmol): IR (KBr pellet) 3420, 3293, 2930, 2886, 1480, 1458, 1379, 1365, 1358, 1298, 1283, 1267, 1096, 968, 928, 860, 777, 756, 742, 708, 625 cm^{-1} ; 1H NMR (D_2O , pD 6.0) δ 2.75–3.28 (18H, m, NCH_2), 5.14 (1H, dd, $J = 10.1, 3.2$ Hz, OCHC), 7.43–7.55 (5H, m, ArH); ^{13}C NMR (D_2O , pD 6.0) δ 45.97, 46.00, 46.2, 48.4, 48.5, 53.7, 55.0, 61.9, 72.4, 128.9, 131.4, 131.8, 114.0; $[\alpha]_D -64.4^\circ$ (c 1.00, H_2O). Anal. Calcd for $C_{16}H_{28}N_4O_3Cl_2 \cdot Zn$: C, 34.5; H, 5.1; N, 10.1. Found: C, 34.7; H, 5.2; N, 10.0.

Preparation of Alkoxide Pendant Attached Zinc(II) Complex with 11 ($14b \cdot ClO_4$). To a solution of $14a \cdot (ClO_4)_2$ (278 mg, 0.50 mmol) in MeOH (11 mL) was added 0.5 mL of 1 M methanolic NaOMe. Colorless solid was precipitated by slow evaporation and recrystallized from aqueous solution (pH 9.5) to obtain $14b \cdot ClO_4$ as colorless prisms in 96% yield (219 mg, 0.48 mmol): IR (KBr pellet) 3295, 2922, 2874, 1489, 1453, 1350, 1144, 1094, 982, 932, 855, 795, 774, 756, 710, 625 cm^{-1} ; 1H NMR (D_2O , pD 9.5) δ 2.69–3.09 (17H, m, NCH_2), 3.22 (1H, ddd, $J = 13.8, 11.1, 4.3$ Hz, NCH_2), 4.86 (1H, t, $J = 6.6$ Hz, OCHC), 7.34–7.49 (5H, m, ArH); ^{13}C NMR (D_2O , pD 9.5) δ 45.2, 46.2, 46.6, 46.8, 47.6, 48.1, 52.6, 54.9, 63.5, 74.3, 129.2, 130.8, 131.6, 146.0; $[\alpha]_D -65.8^\circ$ (c 1.00, H_2O). Anal. Calcd for $C_{16}H_{27}N_4O_3ClZn$: C, 42.1; H, 6.0; N, 12.3. Found: C, 42.4; H, 6.0; N, 12.2.

Synthesis of (S)-1-(2-(4-Nitrophenylphosphoryl)-2-phenylethyl)-1,4,7,10-tetraazacyclododecane ($16a \cdot ClO_4$). A DMF solution (8 mL) of $14b \cdot ClO_4$ (91.3 mg, 0.20 mmol) and bis(4-nitrophenyl) phosphate sodium salt (72.4 mg, 0.20 mmol) was stirred at 35 °C for 1 day. After the solvent was evaporated, the residue was dissolved in water (50 mL) and the pH was adjusted to 6.0 with 0.1 M aqueous $HClO_4$. The aqueous solution was washed with diethyl ether (15 mL \times 3) and

(22) (a) Morrow, J. R.; Trogler, W. C. *Inorg. Chem.* **1988**, *27*, 3387–3394. (b) Kirby, A. J.; Younas, M. *J. Chem. Soc. B* **1970**, 1165–1172.

evaporated to dryness. The residue was recrystallized from water to obtain **16a**·ClO₄ as colorless prisms (98 mg, 0.15 mmol, 73% yield): dec 175°; IR (KBr pellet) 3303, 2934, 2885, 1611, 1591, 1514, 1493, 1458, 1346, 1252, 1146, 1090, 916, 864, 793, 754, 741, 700, 625, 550 cm⁻¹; ¹H NMR (D₂O, pD 6.5) δ 2.93–3.30 (17H, m, NCH₂), 3.37 (1H, dd, *J* = 15.3, 9.8 Hz, NCH₂), 5.47 (1H, m, OCH), 7.02 (2H, dtd, *J* = 9.3, 2.0, 0.9 Hz, OArHNO₂), 7.33–7.46 (5H, m, CArH), 8.05 (1H, dtd, *J* = 9.3, 2.0, 0.6 Hz, OArNO₂); ¹³C NMR (D₂O, pD 6.5) δ 45.6, 45.7, 46.9, 47.0, 47.8, 47.9, 53.3, 56.7, 65.1 (*J*_{PC} = 5.9 Hz), 80.2 (*J*_{PC} = 6.6 Hz), 123.0 (*J*_{PC} = 5.1 Hz), 128.4, 129.1, 131.6, 131.7, 140.3, 146.5, 159.0 (*J*_{PC} = 5.9 Hz); ³¹P NMR (D₂O, pD 6.5) δ -3.59 (*J*_{HP} = 9.2, 2.7 Hz); [α]_D -43.2° (*c* 1.00, MeOH). Anal. Calcd for C₂₂H₃₃N₅O₁₁ClPZn: C, 39.1; H, 4.9; N, 10.4. Found: C, 38.9; H, 4.9; N, 10.4.

Syntheses of Racemic Ligand and Its Zn^{II} Complexes. The racemic dioxocyclen derivative was prepared by the same method as that for **13** using *rac*-styrene oxide to give colorless prisms in 43% yield. Mp, TLC, IR, and NMR are the same as those for **13**.

Using this dioxocyclen derivative, the racemic ligand (cyclen derivative) was prepared by the same method as **11** to give colorless needles as its tetrahydrochloric acid salts in 60% yield. Dec, IR, and NMR are the same as those for **11**·4HCl. [α]_D = 0° (*c* 1.00, H₂O). Anal. Calcd for C₁₆H₃₂N₄OCl₄·1/2H₂O: C, 43.0; H, 7.44; N, 12.5. Found: C, 43.0; H, 7.41; N, 12.1.

The pendant alcohol undissociated Zn^{II} complex with the racemic ligand was prepared by the same method as that for **14a** using the racemic ligand to give colorless prisms as its diperchlorate salts in 93% yield. IR and NMR are the same as those for **14a**·(ClO₄)₂. [α]_D = 0° (*c* 1.00, H₂O). Anal. Calcd for C₁₆H₂₈N₄O₉Cl₂Zn: C, 34.5; H, 5.1; N, 10.1. Found: C, 34.8; H, 5.2; N, 10.1.

Using this Zn^{II} complex, the alkoxide pendant attached Zn^{II} complex was prepared with the same method as that for **14b** to give colorless prisms as perchlorate salts in 90% yield. IR and NMR are the same as those for **14b**·ClO₄. [α]_D = 0° (*c* 1.00, H₂O). Anal. Calcd for C₁₆H₂₇N₄O₅ClZn: C, 42.1; H, 6.0; N, 12.3. Found: C, 42.0; H, 6.3; N, 12.3.

Crystallographic Study. A colorless prismatic crystal of **14b**·ClO₄ (0.40 × 0.40 × 0.20 mm) was used for data collection. The lattice parameters and intensity data were measured on a Rigaku AFC7R diffractometer with graphite-monochromated Cu Kα radiation and a 12-kW rotating anode generator. The structure was solved by a Patterson orientation/translation search and expanded using Fourier techniques. The non-hydrogen atoms were refined anisotropically. Hydrogen atoms were included but not refined. The final cycle of full-matrix least-squares refinement was based on 2862 observed reflections (*I* > 3.00σ(*I*)) to give *R* = 0.050 and *R*_w = 0.077. All calculations were performed using the teXsan crystal structure analysis package developed by Molecular Structure Corp. (1985 and 1992).

Potentiometric pH Titration. The preparation of the test solutions and the calibration method of the electrode system were described earlier.^{10,13} All test solutions (50 mL) were kept under an argon (>99.999% purity) atmosphere at 25.0 ± 0.1 °C with *I* = 0.10 (NaClO₄) and 35 ± 0.1 °C with *I* = 0.10 (NaNO₃). The potentiometric pH titrations were carried out at [total ligand] = 1 mM in the presence or absence of equimolar ZnSO₄, and [total Zn^{II} complex] = 1 mM, and at least three independent titration were made. The calculation methods for ligand protonation constants (*K*_n), Zn^{II} complexation constants (*K*(ZnL)), and the deprotonation constant of the Zn^{II} complex (*K*_a) were the same as described previously.^{10,13} The protonation constants *K*_n are defined as [H_nL]/([H_{n-1}L][H⁺]), the 1:1 metal complexation constant *K*(ZnL) as [ZnL]/([Zn^{II}][L]), and the deprotonation constant *K*_a as [ZnH₋₁L][H⁺]/[ZnL]. The used values of *K*_w' (= [H⁺][OH⁻]) and *f*_{H⁺} were 10^{-13.79} and 0.825 at 25 °C and 10^{-13.48} and 0.823 at 35 °C, respectively.

Kinetics Procedure for the Phosphodiester Cleavage Reaction with Zinc(II) Complexes in Aqueous Solution. The phosphodiester cleavage reaction (i.e., 4-nitrophenolate release reaction) rates of bis-(4-nitrophenyl) phosphate (BNP⁻) and ethyl 4-nitrophenyl phosphate (NEP⁻) were measured by an initial slope method (following the increase in 400-nm absorption of released 4-nitrophenolate) in aqueous solution at 35.0 ± 0.5 °C. Buffer solutions containing 20 mM Good's

buffer (MES, pH 6.0; MOPS, pH 7.0; HEPES, pH 7.4; EPPS, pH 7.9; TAPS, pH 8.4; CHES, pH 9.3; CAPSO, pH 10.0) were used, and the ionic strength was adjusted to 0.10 with NaNO₃ (ca. 90 mM). For the initial rate determination, the following typical procedure was employed: BNP⁻ (10, 5.0, and 2.5 mM) and **14b** (2.0, 1.0, and 0.50 mM) were mixed in the buffered solution, the UV absorption increase recorded immediately and then followed generally until ca. 0.1% formation of 4-nitrophenolate, where log ε values for 4-nitrophenolate were 3.23 (pH 6.0), 3.94 (pH 7.0), 4.11 (pH 7.4), 4.20 (pH 7.9), 4.24 (pH 8.4), 4.26 (pH 9.3), and 4.26 (pH 10.0) at 400 nm. The observed first-order rate constant *k*_{obsd} (s⁻¹) was calculated from the decay slope (4-nitrophenolate release rate/[BNP⁻]). The value of *k*_{obsd}/[total Zn^{II} complex] gave the second-order rate constant *k*'_{BNP} (M⁻¹ s⁻¹) for BNP⁻ hydrolysis. The second-order rate constant *k*_{BNP} was determined from the maximum *k*'_{BNP} values.

The second-order rate constants, *k*_{BNP} and *k*_{NEP}, for Zn^{II}-*N*-methylcyclen **15b** were determined by the same method for that for **14b** with BNP⁻ (10, 5.0, and 2.5 mM) and **15b** (16, 8.0, and 4.0 mM) and NEP⁻ (20, 10, and 5.0 mM) and **15b** (20, 10, and 5.0 mM), respectively.

Kinetics Procedure for the Phosphodiester Cleavage Reaction with 14b in DMF. The phosphodiester cleavage rate of bis(4-nitrophenyl) phosphate (BNP⁻) was measured by an initial slope method (following the increase in 430-nm absorption of released 4-nitrophenolate) in DMF at 35.0 ± 0.5 °C. For the initial rate determination, the following procedure was employed: BNP⁻ (1.0, 0.50, and 0.25 mM) and **14b** (0.20, 0.10, and 0.050 mM) were mixed in DMF, the UV absorption increase recorded immediately and then followed generally until ca. 1% formation of 4-nitrophenolate, where log ε of 4-nitrophenolate was 4.45 at 430 nm. The second-order rate constant *k*_{BNP} in DMF was determined by the similar method for *k*_{BNP} in aqueous solution.

Kinetics Procedure for Intramolecular Hydrolysis with 16b. The hydrolysis (i.e., 4-nitrophenolate release reaction) rate of **16b** was measured by an initial slope method (following the increase in 400-nm absorption of released 4-nitrophenolate) in aqueous solution at 35.0 ± 0.5 °C. Buffer solutions containing 20 mM Good's buffer (HEPES, pH 7.4; EPPS, pH 7.9; TAPS, pH 8.3 and 8.6; CHES, pH 9.1 and 9.5; CAPSO, pH 10.0; CAPS, pH 10.5) were used, and the ionic strength was adjusted to 0.10 with NaNO₃ (ca. 90 mM). For the initial rate determination, the following procedure was employed: **16b** (1.0, 0.50, and 0.25 mM) were mixed in the buffered solution, the UV absorption increase recorded immediately and then followed generally until ca. 1% formation of 4-nitrophenolate, where log ε values of 4-nitrophenolate were 4.11 (pH 7.4), 4.24 (pH 8.3), 4.25 (pH 8.6), 4.26 (pH 9.1), 4.26 (pH 9.5), 4.26 (pH 10.0), and 4.27 (pH 10.5). The first-order rate constant *k*'_{PDE} (s⁻¹) was calculated from the decay slope. The first-order rate constant *k*_{PDE} (s⁻¹) was obtained from the maximum *k*'_{PDE}.

Acknowledgment. We are thankful to the Ministry of Education, Science and Culture in Japan for financial support by a Grant-in Aid for Science Research (A) (No. 04403024) for E.K. and by a Grant-in-Aid for Encouragement of Young Scientists (No. 06857180) for T.K. NMR instruments in the Research Center for Molecular Medicine (RCMM) in Hiroshima University were used.

Supporting Information Available: Text describing experimental details for crystallographic study, and listings of crystallographic parameters, atomic coordinates, anisotropic displacement parameters, bond lengths, bond angles, torsion angles, and nonbonded contacts for **14b**·ClO₄ (30 pages); listing of observed and calculated structure factors for **14b**·ClO₄ (20 pages). This material is contained in many libraries on microfiche, immediately follows this article in the microfilm version of the journal, can be ordered from the ACS, and can be downloaded from the Internet; see any current masthead page for ordering information and Internet access instructions.